Tellus (2006), 58B, 293–304
Printed in Singapore. All rights reserved

TELLUS

Water vapour $^{18}O/^{16}O$ isotope ratio in surface air in New England, USA

By XUHUI LEE[1*], RONALD SMITH[2] and JOHN WILLIAMS[2], [1]*School of Forestry and Environmental Studies, Yale University, New Haven, CT, USA;* [2]*Department of Geology and Geophysics, Yale University, New Haven, CT, USA*

(Manuscript received 9 December 2005; in final form 27 March 2006)

ABSTRACT

In this paper, we report the results of the analysis of two high-resolution time-series of water vapour $^{18}O/^{16}O$ ratio (δ_v) in surface air observed in Connecticut, USA. On an annual time-scale, δ_v is a linear function of $\ln w$, where w is water vapour mixing ratio, and is approximated by a Rayleigh distillation model with partial (80%) rainout. On time scales a few days, δ_v shows considerable variations, often exceeding 20 per mil, and is higher in the wetting phase than in the drying phase of a weather cycle. In precipitation events, the vapour in the surface layer is in general brought to state of equilibrium with falling raindrops but not with snowflakes. On a diurnal time-scale, a peak-to-peak variation of 1–2 per mil is observed at a coastal site. At an interior site, evidence of a diurnal pattern is present only on days of low humidity. Our results suggest that the intercept parameter of the Keeling plot is an ambiguous quantity and should not be interpreted as being equivalent to the isotopic signature of evapotranspiration.

1. Introduction

The objective of this study is to investigate meteorological and ecological mechanisms that influence the ^{18}O composition of water vapour in surface air near the ground. The advance in in-situ technology has made it possible to measure the vapour ^{18}O:^{16}O isotope ratio δ_v[1] at high temporal resolution and on a continuous basis (Lee et al., 2005). Such measurement offers unique opportunities to examine the temporal variations in δ_v and gain insights into the mechanisms involved.

Investigation of this kind is of interest to the atmospheric and ecological communities for two main reasons. First, there is considerable interest in the use of atmospheric $C^{18}O^{16}O$ as a tracer for resolving the role of the terrestrial biosphere in the global carbon cycle. It has been long recognized that biospheric exchange of ^{18}O–CO_2 with the atmosphere is tightly coupled with the exchange of ^{18}O–H_2O (Francey and Tans, 1987). Fractionation associated with transpiration and evaporation enriches the leaf and soil water with ^{18}O, which in turn causes the CO_2 that diffuses back out of the leaf and the soil to be enriched with ^{18}O (Farquhar et al., 1993). The degree of enrichment depends on, among other things, δ_v in surface air (Dongmann et al., 1974; Roden and Ehleringer, 1999). In situations where direct measurement of δ_v is not available, model calculations of the enrichment often assume a constant δ_v value. Errors associated with the assumption can be systematic because δ_v covaries with other meteorological variables, especially air humidity (White and Gedzelman, 1984; He et al., 2001; Lee et al., 2005), that drives the model calculation. Actual measurement of δ_v will improve these calculations.

Secondly, it has been suggested that temporal variations in δ_v and water vapour mixing ratio, w can be used to infer the isotopic composition of evapotranspiration (ET) via the Keeling plot approach (Keeling, 1958). Implicit in the Keeling approach are the assumptions that the temporal variations are attributable to a single source and that the source isotopic signal is constant over the observational period. However it is well known that in addition to surface ET, other factors can cause temporal variations in δ_v (Fig. 1). So far, it is virtually impossible to isolate these other factors from the real ET signal because of the small data samples involved in almost all the published studies on this topic.

The high-time resolution, continuous measurement of δ_v presents a new opportunity for the study of the hydrological cycle and the associated atmospheric processes, especially those involving the phase changes of water. In Fig. 1, it is proposed that δ_v in surface air is influenced by air mass advection, ET

[1]Following the usual convention, the ^{18}O abundance is expressed in delta-notation in reference to VSMOW

$$\delta_v = (R_v/R_{\mathrm{Vsmow}} - 1) \times 1000 \text{ per mil}$$

where R_v is the ^{18}O:^{16}O molar ratio of water vapour and R_{vsmow} ($= 0.0020052$) is the standard molar ratio (VSMOW).

*Corresponding author.
e-mail: xuhui.lee@yale.edu
DOI: 10.1111/j.1600-0889.2006.00191.x

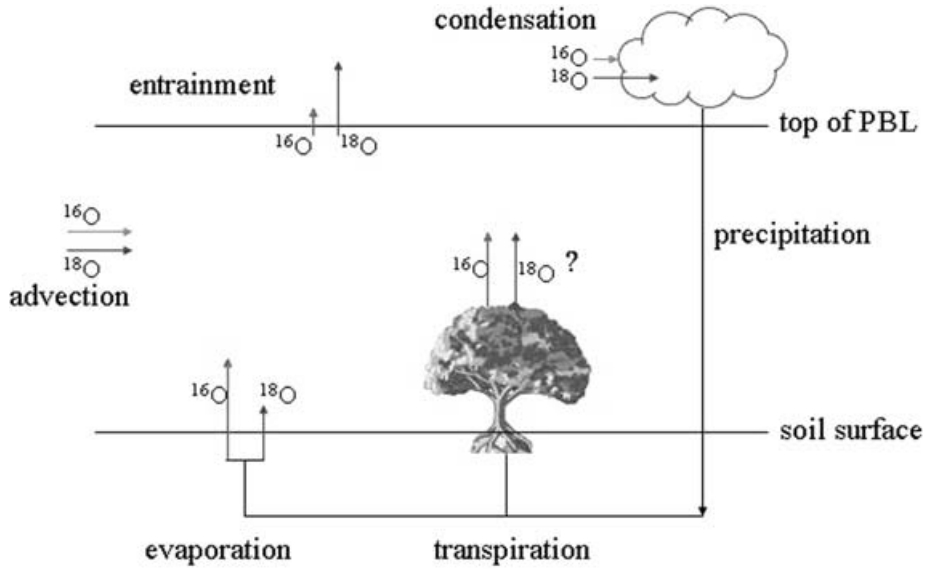

Fig. 1. Schematic diagram of processes influencing the isotopic composition of water vapour in surface air. Arrows of unequal length indicate processes that fractionate ^{18}O and ^{16}O.

at the surface, entrainment at the interface between the free atmosphere and the boundary layer, in-cloud condensation and precipitation. Some of these factors can be understood through the lens of idealized processes whose physics has been well established. A classic of these is the Rayleigh distillation theory for an open system in which a fraction of water vapour is condensed into the liquid phase and is immediately rained out. As the vapour mixing ratio decreases due to rainout, the vapour ^{18}O content becomes progressively lower. The theory can be viewed as an idealized representation of drying that accompanies the advection of an air mass from its vapour source region. Although difficult to apply to individual weather cycles because condensation temperature and the vapour source regions are not known precisely, it is a reasonable framework for the interpretation of seasonal changes in δ_v (e.g. Jacob and Sonntag, 1991).

A second idealized process describes a closed system where liquid and vapour phases of water reach the state of equilibrium. The equilibrium state, the norm in warm clouds (Jouzel, 1986), is never fully reached near the ground in dry weather, but its mathematical representation can serve as an end member of the actual δ_v value on seasonal time-scales (Section 3.1). During a prolonged rain event, vapour in surface air can potentially reach equilibrium with the falling liquid droplets (Steward, 1975). Thus, a simple equilibrium calculation can be performed to predict δ_v from that of rainwater, and vice versa.

A third idealized process involves the problem of evaporation from an open water body, the physics of which is captured by the model put forth by Craig and Gordon (1965). The principles of the Craig–Gordon model have been extended to the less-ideal, terrestrial environment to quantify the isotopic exchange of water vapour with soil (Riley, 2005) via evaporation and leaves (Dongmann et al., 1974; Flanagan et al., 1991) via plant transpiration. The calculated isotope composition of soil evaporation is extremely sensitive to relative humidity in air: It can be −30 per mil lower than that of the soil water when air is dry, and similar or even greater than the latter when air is near saturation. This may be an important point in the context of this study. Since a repeatable diurnal pattern exists in relative humidity, there may exist a diurnal signal in δ_v in surface air as a result of the diurnal change in the evaporation isotope signal.

On the diurnal time-scale, δ_v in surface air may also be influenced by other local factors such as entrainment of the free atmosphere to the convective boundary layer. Conceptually, the entrainment process can be viewed as a continuous turbulent exchange of vapour between the drier free atmosphere above the boundary layer and the more moist boundary layer. Because a large difference exists in the vapour isotope ratio between the two air layers (He and Smith, 1999), the entrainment process can play a role in the ^{18}O budget of the boundary layer. The extent of this role is however not known at present. Isotopic measurements may offer constraints on the entrainment rate and boundary layer budget calculations of surface fluxes.

The above discussion follows a reductionist reasoning and is somewhat overly simplistic. A much improved realism is offered by sophisticated global- and regional-scale modeling studies of water isotopes, which have integrated the relevant processes (Hoffmann et al., 1998; Cuntz et al., 2003; Sturm et al., 2005). These models have been validated against data on the condensed phases but rarely against data on the vapour phase. The data reported by this study can potentially be used in this regard.

In this paper, we will characterize variations in δ_v on various time-scales including season, weather cycle, rain shower and

Fig. 2. Map showing the location of the measurement sites. The width of the state of Connecticut is 140 km.

diurnal time-scales and discuss mechanisms that contribute to the variations. A central part of the study is two nearly continuous time-series of δ_v observed in Connecticut at hourly intervals from December 2003 to December 2004 and from May to October 2005. Statistical analysis and simple physical models are used to aid the data interpretation. Our discussion, guided by the roadmap shown in Fig. 1, makes the implicit assumption that processes that operate on different time-scales can be isolated from each other.

2. Data[2]

2.1. The New Haven experiment

From December 2003 to December 2004, the measurement of water vapour isotope ratio, δ_v, and mixing ratio, w, was made in New Haven, Connecticut (41.31°N 72.92°W, elevation 20-m above mean sea level) with a tunable diode laser (TDL) trace gas analyser (Fig. 2). The principle of operation and calibration procedure were described in Lee et al. (2005). Briefly, air was drawn from the rooftop of our laboratory building into the TDL manifold. At the inlet of the sampling tube was a heated 0.67-L buffer volume. Also drawn to the manifold were ultra high-purity nitrogen gas (zero gas) and moist air (span gas) whose isotope content was known. Thespan gas mixing ratio was controlled to match that of the ambient air to within 10%, minimizing the water vapour pressure broadening effects and a nonlinearity problem. At any given time, only one manifold port was connected to the TDL sample cell and the rest were bypassed. A full manifold switching cycle took 80 s. Calibration of δ_v was made for every switching cycle according to Lee et al. (2005). The 80-s measurement was averaged to produce hourly mean values. Precision of the hourly data was 0.2 per mil at a w value of 2.67 mmol mol^{-1} (dewpoint temperature of -10.8°C at sea level) and improved to 0.1 per mil at 15.3 mmol mol^{-1} (dewpoint temperature 13.4°C).

An infrared analyser (model 6262, LiCor, Inc., Logan, UT) was used to monitor, in parallel to the TDL system, the span gas water vapour mixing ratio. The H_2O gain factor produced by the redundant measurement was used to correct the TDL measurement of the ambient water vapour mixing ratio. In the following, water vapour mixing ratio w is expressed as molar fraction in mmol mol^{-1}. To convert molar mixing ratio to mixing ratio by weight, we note that 1 mmol mol^{-1} = 0.622 g kg^{-1}.

Axillary data (wind speed, direction, temperature, relative humidity, precipitation time and amount) were obtained from the US National Service, at the Tweed Airport Station (station ID 065273), 7 km to the SE of our laboratory. Precipitation water was collected at a site 6 km N of the laboratory. The ^{18}O analysis of the precipitation samples was event-based and was performed in triplicate by the CO_2 equilibration technique (Iso-Analytical Limited, Sandbach, Cheshire, UK). The equilibrated CO_2 was analysed by continuous flow using a Europa Scientific ANCA-G and Hydra 20-20 IRMS. The sample was measured against three reference standards traceable to the primary reference standards VSMOW and SLAP (Standard Light Antarctic Precipitation) distributed by the IAEA, Vienna.

2.2. The Great Mountain experiment

In the spring of 2005, the TDL system was moved to the Great Mountain Forest, Norfolk, Connecticut (41°58′N, 73°14′W, elevation 460 m above mean sea level). The experiment started in mid-May and continued till the end of October. A detailed description of the experimental set-up is given elsewhere. A few important points are reproduced here for the reader's convenience. Air was drawn from two heights roughly 3 and 13 m above the treetops though heated tubings to the TDL analyzer housed in an air-conditioned hut near the measurement tower. Only data for the lower intake were reported here. Two span gases with identical vapour isotope content were deployed for calibration, one with a vapour mixing ratio roughly 5% higher and the other 5% lower than the ambient mixing ratio. Calibration of δ_v was accomplished by interpolation against these two span gases to further minimize the nonlinearity problem. Auxiliary data were obtained with instruments mounted on the tower (Lee and Hu, 2002). Rain water was collected at the site for isotopic analysis.

[2] The full data set is available at http://pantheon.yale.edu/∼xhlee/.

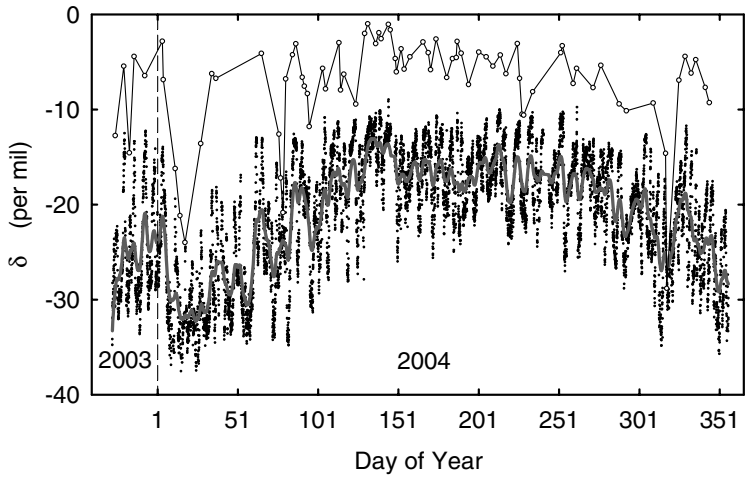

Fig. 3. Hourly value of the isotope composition of water vapour in New Haven, December 2003 to December 2004 (dots). Also shown are a 10-d moving average of the vapour isotope ratio (grey line) and precipitation isotope ratio (circles).

Table 1. Monthly mean values of water vapour mixing ratio (w), surface air temperature (T), total precipitation (P), isotope ratios of water vapour (δ_v), precipitation (δ_p) and the vapour in equilibrium with precipitation water ($\delta_{v,e}$), and linear correlation coefficients of δ_v with T (r_T) and w (r_w), from December 2003 to November 2004 in New Haven, and June to October 2005 at the Great Mountain Forest. The monthly δ_p was computed as the precipitation weighted mean value.

Month/Year	w (mmol mol^{-1})	T (°C)	P (cm)	δ_v (per mil)	δ_p (per mil)	$\delta_{v,e}$ (per mil)	r_T	r_w
			New Haven					
12/03	4.9	1.6	10.6	−24.9	−9.4	−20.7	0.56	0.86
1/04	2.9	-5.5	5.7	−29.4	−14.3	−26.3	0.77	0.91
2/04	3.2	−0.3	6.6	−28.4	−6.6	−18.2	0.23	0.76
3/04	5.4	3.9	20.1	−22.5	−9.0	−20.1	0.37	0.77
4/04	7.7	8.9	25.0	−19.5	−7.8	−18.4	0.39	0.84
5/04	13.0	14.8	7.2	−15.1	−5.1	−15.2	0.20	0.83
6/04	15.3	18.9	2.8	−16.5	−4.8	−14.6	0.09	0.82
7/04	19.6	22.0	12.0	−16.6	−5.9	−15.4	0.02	0.81
8/04	19.9	21.2	12.6	−16.6	−8.4	−17.9	0.57	0.84
9/04	16.3	19.0	23.8	−17.4	−6.0	−15.7	0.28	0.71
10/04	10.0	11.9	4.9	−19.8	−9.8	−19.7	0.23	0.70
11/04	7.1	7.7	8.6	−22.8	−4.4	−20.1	0.58	0.89
			Great Mountain					
6/05	18.4	19.4	6.2	−17.1	−9.1	−18.8	0.48	0.68
7/05	19.9	20.6	7.3	−17.2	−7.8	−17.4	0.37	0.81
8/05	20.0	20.7	8.2	−16.6	−4.6	−14.2	0.49	0.93
9/05	15.6	17.7	4.1	−17.7	−3.8	−13.7	0.57	0.75
10/05	13.8	14.2	37.8	−19.9	−7.6	−17.7	0.78	0.83

3. Results and discussion

3.1. Seasonal variations

3.1.1. General pattern. Figure 3 presents a time-series plot of all valid hourly observations of δ_v in New Haven, from December 2003 to December 2004. Over periods shorter than one month, considerable variations occurred, sometimes exceeding 20 per mil over just a few days. Much of the variations was caused by advection of air mass in varying stages of rainout history (Section 3.3). A similar pattern was observed at the Great Mountain (data not shown). Table 1 summarizes monthly mean statistics for both sites. In general, δ_v was higher in the warm season (May–October) than in the cold season (November–April). The observed maximum and minimum hourly δ_v values in New Haven were approximately −10 and −38 per mil, respectively. The highest monthly mean value occurred in May, 2004 (−15.1 per mil) and the lowest monthly mean in January 2004 (−29.4 per mil). The

annual mean for New Haven was −20.8 per mil, slightly lower than the 7-yr average of −18.9 per mil reported for Heidelberg, Germany (Jacob and Sonntag, 1991).

For practical purposes, it is useful to examine the correlation of δ_v with other meteorological variables. In the past, variations in water isotope ratios were often explained in terms of temperature variations. When all the data in Fig. 3 were considered, the linear correlation coefficient between δ_v and surface temperature was 0.73. On a monthly basis, the correlation coefficient varied from 0.02 to 0.78, with stronger correlation found in the cold season (Table 1). In general, temperature was a poor predictor of δ_v. In comparison, a much better correlation existed with water vapour mixing ratio w. Over monthly intervals, the linear correlation with w was in the range of 0.68 to 0.93. The w correlation for the full year New Haven data was log-linear, as shown in Fig. 4. The regression equation

$$\delta_v = -35.02 + 6.84 \ln(w) \quad (1)$$

captured 78% (coefficient of variations $R^2 = 0.78$; confidence level <0.001) of the observed variation in δ_v (Fig. 4, solid line).

3.1.2. Comparison with model calculations. The dependence of δ_v on air humidity can be partially explained by the principle of Rayleigh distillation for air mass advection. As moist air migrates away from its source region, some water condenses from the vapour form to the liquid and solid form and precipitates out. Since the condensed phases are enriched with ^{18}O relative to the vapour phase, the removal of water by precipitation will decrease both w and δ_v. In the special case where water in the condensed phase is removed immediately, a condition achieved in an open system, condensation occurs at a constant temperature, and water originates from a single source at one instant, the following relationship holds (e.g. Gat, 1996):

$$\delta_v = \delta_{v,o} + (\alpha - 1) \ln(w/w_o), \quad (2)$$

where w_o and $\delta_{v,o}$ are water vapour mixing ratio and isotope ratio at the source, respectively, and α represents the equilibrium fractionation factor, expressed as a function of temperature at which condensation occurs (Jouzel, 1986). Equation (2) is a linearized form of the original Rayleigh equation, with the higher order terms being ignored. A comparison of eq. (2) with the data is given in Fig. 4 (long-dashed line). The calculation was made with a condensation temperature of 0°C, w_o of 30 mmol mol^{-1}, and $\delta_{v,o}$ of −10 per mil. The theoretical prediction captures the observed log-linear pattern but underestimates the actual vapour isotope ratio. Forcing a good fit with the data would require an unrealistic condensation temperature of 20°C. Despite this significant discrepancy, that both modelled and observed relationships were log-linear lends some support to our interpretation that on an annual time-scale, temporal variations in δ_v were dominated by Rayleigh distillation that accompanies the advection of an airmass from its vapour source region.

For comparison, model calculation is also presented in Fig. 4 for a closed system where the vapour and water in the condensed phase co-exist in equilibrium, as

$$\delta_v = \delta_{v,o} - \ln[(1 - \alpha)w/w_o + \alpha]. \quad (3)$$

This model is not log-linear. Calculation based on this model appears reasonable in the wet range ($w > 15$ mmol mol^{-1}) but grossly overestimates δ_v when air is dry (dash-dotted line, Fig. 4). This is expected because the model requires that the vapour and liquid forms of water obey the equilibrium state, which is not a valid condition when the air is not saturated.

Clearly, an airmass is neither a fully open nor fully closed system. When condensation occurs, some but not all of water in the condensed phases will rain out. Assuming that the rainout fraction (f) is constant throughout the lifespan of the airmass, mass balance consideration leads to (Appendix A)

$$\delta_v = \delta_{v,o} + \frac{\alpha - 1}{1 - \alpha(1 - f)} \ln\{[1 - \alpha(1 - f)]w/w_o + \alpha(1 - f)\}. \quad (4)$$

In the limits $f \to 0$ and 1, eq. (4) is simplified to eqs. (3) and (2), respectively. Figure 4 presents the model calculation with a rainout fraction $f = 0.8$ (dashed line). Even though not perfect, this model with partial rainout does a much better job than the idealized models of fully open and fully closed systems.

3.1.3. Comparison with the published data. In Fig. 5, the regression equation (eq. 1) is compared with several datasets found in the literature. For clarity, the data in Fig. 4 is reproduced here as a regression line. Our data stood in sharp contrast with

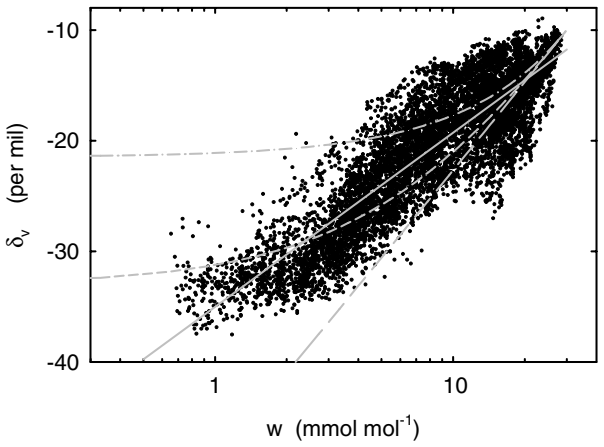

Fig. 4. A log-linear plot of the vapour isotope ratio, δ_v against the vapour molar mixing ratio, w, New Haven, December 2003 to December 2004. Least-squares regression of the data is given by the solid line ($\delta_v = 6.84 \ln(w) - 35.02$, $R^2 = 0.78$). Also shown are theoretical values based on models for an open system (long-dashed line), a two-phase closed system (dash–dotted line) and a two-phase system with partial (80%) rainout (short-dashed line). All theoretical calculations are made with a temperature of 0°C, and mixing ratio and isotope ratio of water vapour of 30 mmol mol^{-1} and −10 per mil at the source.

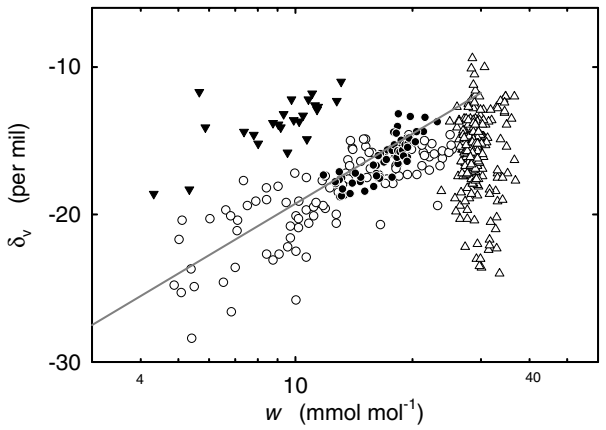

Fig. 5. A comparison of the data of this study (straight line) with the published data on the vapour isotope composition near the Earth's surface: solid triangle, surface air over the Mediterranean Sea (Gat et al., 2003); open circle, monthly mean values for Heidelberg, Germany (Jacob and Sonntag, 1991); open triangle, surface air over tropical and subtropical oceans (Lawrence et al., 2004); bullet, hourly observation in Utah, USA (Lee et al., 2005).

those reported for the tropical region where mixing ratio was a poor predictor of δ_v. Lawrence et al. (2004) found that the highest δ_v values approached isotopic equilibrium with seawater during quiescent weather or in regions of isolated convection and lowest values occurred downwind of major weather disturbances, even though the surface w did not differ much between these two endpoints. The lack of correlation with w may have been related to their air trajectory pattern, which lay most of the time over the tropical ocean. We suspect that one of the assumptions of the Rayleigh distillation model—that water vapour originates at a single instant from its source—was no longer satisfied.

With the exception of Lawrence et al. (2004), other studies generally showed that w was a good predictor for δ_v in surface air (see also White and Gedzelman, 1984; He et al., 2001; Williams et al., 2004). At a given w level, the isotope content of vapour over the Mediterranean Sea was higher than over land. Our observation was broadly consistent with the monthly data for Heidelberg, Germany (Jacob and Sonntag, 1991) and our previous observation at an interior location in the continental US (Lee et al., 2005).

3.2. Water vapour and precipitation isotope ratios

3.2.1. Relationship for monthly mean values. In addition to w, isotope ratio of local precipitation, δ_p, can be used to build statistical relationship for δ_v. This approach is attractive because information on the precipitation isotope ratio is readily available. Using monthly mean data for New Haven, the linear correlation between δ_v and δ_p was 0.58. The correlation improved to 0.81 if instead of δ_v the isotope ratio of vapour in equilibrium with the precipitation water, $\delta_{v,p}$, was used for the calculation (Table 1). The linear regression with $\delta_{v,e}$ is given by (New Haven data only; confidence level <0.01)

$$\delta_v = 1.20\delta_{v,e} + 1.41 \quad R^2 = 0.64. \tag{5}$$

The larger-than-unity slope reflects the fact that $\delta_{v,e}$ was higher than and similar to δ_v in the cold and warm season, respectively. The result did not deviate too much from that of Jacob and Sonntag (1991) who reported a slope of 1.11 and an intercept value of 1.56 per mil for the same type of regression. Simulations of a global circulation model give a δ_v that is roughly 10 per mil lower than that of precipitation water (Hoffmann et al., 1998; Cuntz et al., 2003), which is in broad agreement with our data (Table 1).

Despite the statistically robust correlation, the theoretical underpinning of such relationship is ambiguous. On a monthly basis, there is no reason why water vapour near the ground should be in equilibrium with precipitation water. In fact, if water vapour in surface air originates completely from the evapotranspiration of precipitation water stored in the soil, δ_v would be identical to δ_p and hence greater than $\delta_{v,e}$. On the other hand, Rayleigh distillation accompanying airmass advection would result in a δ_v value lower than δ_p. It is fortuitous that these two opposing factors compensated each other to the extent such that similar monthly δ_v and $\delta_{v,e}$ values were observed, especially in the warm season.

3.2.2. Equilibrium during precipitation events. During periods of rainy weather, the vapour may reach equilibrium with the falling rainwater. The evaporation of the falling raindrops will generally cause their ^{18}O content to increase and at the same time increases the humidity of the air near the ground. In prolonged rain events, the humidity will reach saturation and it is postulated that at such time the equilibrium state should prevail (Steward, 1975). The equilibrium state was first confirmed by Steward (1975) by simulating rainfall in a chamber filled with saturated air. Evidence of the equilibrium state in the real atmosphere was provided by Lawrence et al. (2004) and others, although their data show considerable scatter due in part to the problem that vapour sampling was intermittent and was not precisely timed with the onset and termination of the rain event. This problem was circumvented by the high-time resolution, continuous measurement in this study.

Figure 6 plots the mean δ_v against $\delta_{v,e}$ observed for all rain events in New Haven from December 2003 to December 2004 and at the Great Mountain Forest from mid-May to mid-September 2005. Here the event-based mean δ_v was computed from the hourly observations and weighted by hourly precipitation amount. The equilibrium value $\delta_{v,e}$ was evaluated at the surface temperature from the isotope ratio of rain water collected over the full event. For most precipitation events, only one sample was collected after the event ended. Rain samples were collected at hourly intervals in four storms. Examination of these samples showed that the time evolution of δ_v tracked very well the change

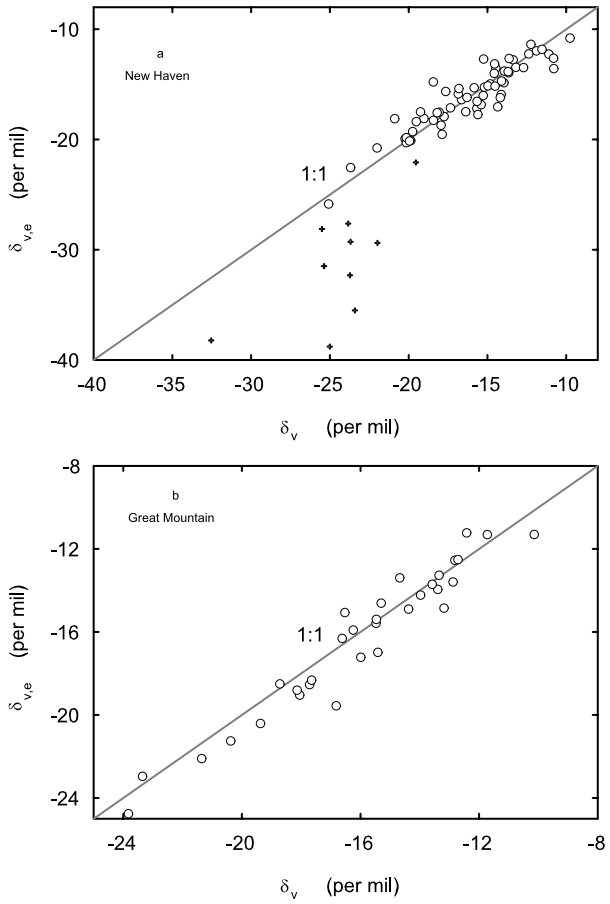

Fig. 6. A comparison of the measured water vapour isotope ratio, δ_v, and the isotope ratio of water vapour in equilibrium with the falling precipitation, $\delta_{v,e}$, during precipitation events in New Haven from December 2003 to December 2004 (a) and Great Mountain Forest from June to October 2005 (b): circle, rain; cross, snow.

in $\delta_{v,e}$ through these storms. The scatter in the New Haven data was slightly larger than the Great Mountain data, because during the New Haven experiment, precipitation amount measurement, precipitation sample collection and δ_v monitoring were not made at the same location (Section 2.1). Ehhalt and Östlund (1970) reported a deviation of D/H from isotopic equilibrium by -20 to $+10$ per mil at an elevation of 600 m above the ground along a transect in a hurricane. They suggested that the sign of the deviation depended on whether the observation was made in the zone of updraft or downdraft. For example, in the zone of downdraft, raindrops that have been formed at higher levels always will exhibit lower isotope content than the value that corresponds to isotopic equilibrium with the environment, especially when their fall speed is large. They did not reported the $^{18}O/^{16}O$ ratio. Their data could be tranformed with the global mean meteoric line to give a $^{18}O/^{16}O$ deviation from equilibrium on the order of -2.5 to 1.2 per mil, which is comparable to the scatter seen in our data. The within-storm heterogeneity is a factor contributing to the scatter in Fig. 6. Overall, the agreement with the equilibrium prediction was excellent when all rain events were considered. Analysis of the residual from the 1:1 line did not reveal any statistically significant correlation with temperature, precipitation amount or duration.

Figure 6 also presents a comparison of δ_v and $\delta_{v,e}$ for snow events. In this case, water vapour near the ground was always heavier than the prediction of equilibrium with the falling snowflakes, sometimes by as much as 15 per mil. This is in contrast to the monthly mean data in the cold season when water vapour was lighter than the equilibrium value (Table 1). The data indicate that the exchange of vapour with the falling snowflakes, which were formed at high altitudes and were much lighter than the surface water vapour, was too slow to bring the surface air to the equilibrium state even though air was saturated during the event.

3.3. Variations through weather cycles

3.3.1. An example of looping. Climatologically, New England is located at the receiving end of almost all storm tracks in North America (Zielinski and Keim, 2003). A typical weather cycle in New England usually lasts 3–10 d and comprises of a wetting phase in which w increases with time as a frontal system approaches the site, bringing moisture from the Atlantic Ocean and the Gulf of Mexico, the passage of a cyclonic system, and a drying phase in which a dry air mass displaces the moist air, causing w to decrease with time. Changes in air moisture level, its source region and rainout history through the weather cycle can cause considerable variability in δ_v (Fig. 3).

Figure 7 presents a detailed view of the temporal variations in w and δ_v through a weather cycle that occurred from 20 to 28 December 2003 (days of year 354 to 362). The isotope ratio reached its lowest value of -33.6 per mil in the late evening of 20 December (day of year 354), and increased steadily with time to the maximum value of -12.2 per mil at 12:00 local standard time (LST) 24 December (day of year 358), in the middle of a rain event, giving a full range of variation of 21.4 per mil over the 5-d period. A total of 15 mm of rain was recorded over this period whose isotope ratio was -6.4 per mil.

When presented in a scatter plot of δ_v versus w, the data revealed an interesting looping or hysteresis pattern: at a given moisture level, δ_v was approximately 5 per mil higher in the wetting phase than in the drying phase. The looping pattern was a common occurrence throughout the year, but was more profound in the winter than in the summer. It was most evident during cold front events and was absent in occluded fronts even though passage of occluded fronts could reduce w by similar amounts. Trajectory analysis revealed that ahead of a cold front, moist air was in general being drawn up from the south (the Atlantic Ocean and the Gulf Mexico), and the $\delta_v - w$ curve appeared to reflect the Rayleigh distillation of this moist airmass and its mixing with the dry airmass left over from a previous weather cycle. After

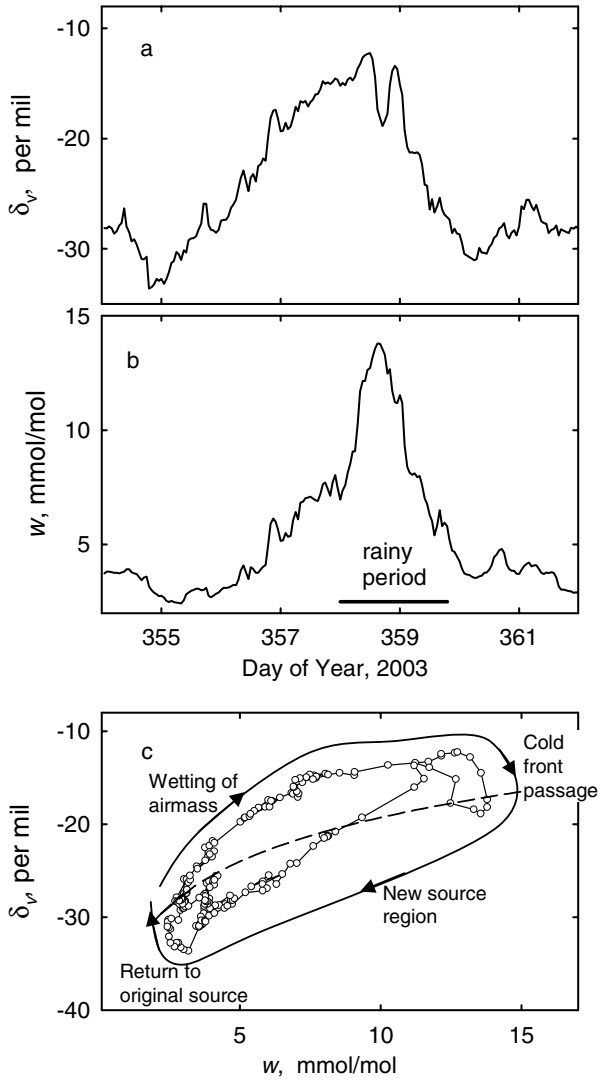

Fig. 7. An example of variations in vapour isotope ratio δ_v and mixing ratio w through a weather cycle, New Haven, 19–26 December 2003 (days of year 354–361). The variations are compared with a regression model based on the full data set (dashed line, panel c; eq. 1). A total of 15-mm rain fell during this period. The isotope ratio of the rainwater was −6.4 per mil. A cold front passed the site on the evening of day 358. Arrows indicate time progression.

the cold front passage, both w and δ_v dropped concurrently, but not in Rayleigh distillation proportions. At this time, the $\delta_v - w$ curve was displaced downward by 3–6 per mil, which was a signature of an alternate source region because air trajectories now originated from the north-west quadrant. In occluded front events, however, air trajectories were very confusing, without a clear change in the pre- and post-front periods.

It is also apparent from Fig. 7 that the regression model based on the full year's data could suffer large uncertainties when applied to time-scales of weeks or shorter. Because condensation

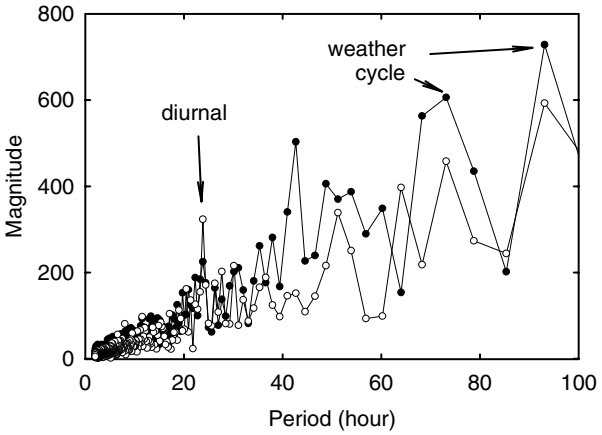

Fig. 8. Comparison of fast Fourier transform results for winter (bullets, January–March) and summer (circles, July–September), New Haven.

temperature and the vapour source regions are not known precisely, simple models of the types discussed above cannot capture the full temporal variations of δ_v in individual weather cycle events. In this sense, the regression equation (eq. 1) should be regarded as a representation of an ensemble mean state of airmass evaporation and condensation history.

3.3.2. Contrast between winter and summer seasons. Figure 8 shows the Fourier transform of the isotope data for two periods, with one in the winter and the other in the summer. Prior to the transform, for missing data points, a simple linear interpolation was done using the values from the hours before and after. In general, the result shows small, random fluctuations in magnitude for less than 24-h periods and larger magnitude of change over longer time-periods of a few days. Specific differences between the seasons can be seen. The summer month plot shows a clear diurnal (24 h) cycle that was larger than the winter signal, while the winter plot shows higher magnitude of variations over longer periods. Variations associated with weather cycles were not limited to a single identifiable period but instead occurred over a broad range of periods greater than 40 h. The stronger signal on the weather cycle time-scale in the winter months is not surprising because cyclonic activity is more active in the cold season.

3.4. Diurnal variations

3.4.1. Magnitude of variations. A 24-h ensemble averaging scheme was used to bring out the diurnal signal. The full dataset from New Haven was broken into four seasons: December–February (winter), March–May (spring), June–August (summer) and September–November (fall). For each period, the hourly observation was grouped into bins and averaged according to time of the day. For convenience of comparison, the mean value of each season was removed from the bin-averaged value. The averaging schedule smoothed out small fluctuations for periods

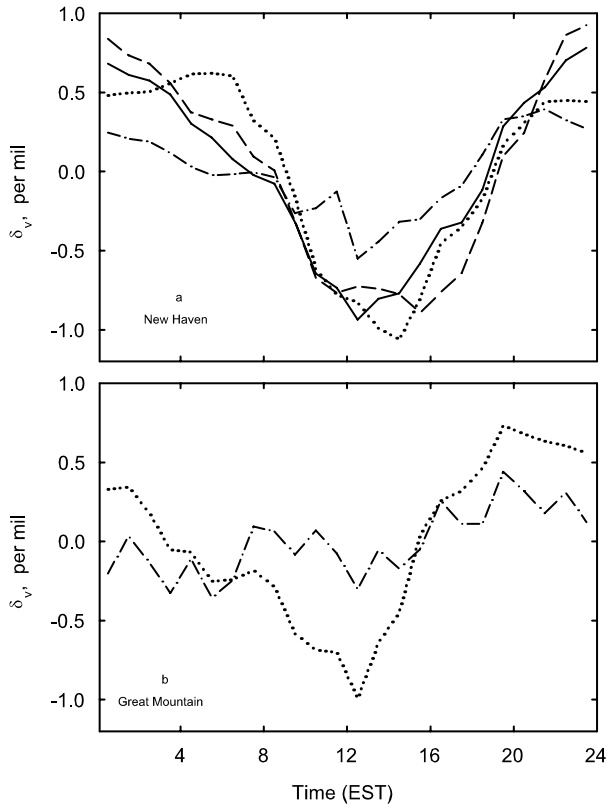

Fig. 9. (a) Twenty-four hour ensemble average values of δ_v for winter (December–February, dash–dotted line), spring (March–May, dotted line), summer (June–August, dashed line) and fall (September–November, solid line), New Haven. (b) Ensemble average for Great Mountain (dash–dotted line, all data from mid-May to mid-September; dotted line, periods with $w < 15$ mmol mol^{-1}).

less than 24 h and also removed the time-trend associated with weather cycles. The result is shown in Fig. 9a. The peak-to-peak variation was 1 per mil in the winter and 2 per mil in the other three seasons. The maximum occurred in the early afternoon hours (12:00–16:00 LST) and minimum around midnight. The seasonal contrast was consistent with the Fourier transform result (Fig. 8). The diurnal pattern was similar to that observed in a temperate forest (Lai et al., 2005) but was different from the observation of Helliker et al. (2002) over a grassland who reported a steady increase of 4 per mil from mid-morning to mid-afternoon on two consecutive days. On average, the diurnal signal was an order of magnitude smaller than the variation through a weather cycle (Fig. 7).

The ensemble averaging scheme was also applied to the Great Mountain data (Fig. 9b), using both the full data set from mid-May and mid-September and a subset of the data that satisfied the condition $w < 15$ mmol mol^{-1}. No obvious diurnal pattern can be found with the full data set. Screening the data for days of low humidity brings out some evidence of diurnal variation, with a peak-to-peak range of roughly 1 per mil.

3.4.2. The role of sea breeze. Because the time-trend associated with airmass advection was eliminated by the ensemble averaging, the remaining diurnal signal was indicative of local influences, such as land–sea breeze circulation, growth and decay of the boundary layer, and surface ET. Located 4 km from the coast of Long Island Sound, the New Haven site was occasionally influenced by the land–sea circulation (Fig. 2). The frequency of sea breeze occurrence was 10–20% in the summer and lower in the winter. On a characteristic sea breeze day, wind direction would switch from NW–NE to SE–SW around 10:00 LST (onset of sea breeze) and would change back to NW–NE around 19:00 LST (onset of land breeze). For comparison, the Great Mountain site was 100 km away from the coastline and was free of the sea breeze influence. The fact that the diurnal pattern was clearly present in New Haven but not easily identifiable at Great Mountain indicates that land–sea breeze circulation plays a dominant role in the diurnal variation of δ_v seen in New Haven. On days with a clearly identifiable sea breeze, a diurnal change of 4 per mil in δ_v was typical, which is several times greater than the ensemble mean values (Fig. 9a).

In the daytime sea breeze phase, air ascends over land, travels across the shoreline, descends to the sea surface and returns to land. As air travels over the water, its vapour isotope content will be modified by the evaporation of seawater. The precise nature of this modification is not known. Craig and Gordon (1965) reported values of -14 to -10 per mil for vapour in the surface layer in the open ocean, which are higher than the typical fair weather values over land (Fig. 4). Similarly, the isotope content of vapour over the Mediterranean Sea was higher than over land (Fig. 5). Both observations contradict our data which show that the vapour ^{18}O content of air blowing from the sea was lower than that of the land air.

We suggest that the sea breeze air, which was recycled at the land–sea interface, might not have fully exchanged its vapour with the sea water. Our observation is consistent, at least in a qualitative sense, with the prediction of the Craig–Gordon model. Using an isotope content of -3.5 per mil for the sea water in Long Island Sound (He, 1998), a typical summertime water surface temperature of 20°C and vapour isotope ratio of -20 per mil, we found that the isotope content of the evaporation flux was extremely sensitive to relative humidity: it took a value of -30 per mil if a relative humidity of 60% was used and increased to -12 per mil at a relative humidity of 80%. The first estimate seems more reasonable since sea breeze usually occurred in anticyclonic conditions, with cool and dry air blowing from Canada, while the second estimate might be more appropriate for the open ocean where relative humidity was on the order of 80% (Pierrehumbert, 1999). Contribution of evaporation of the sea water should therefore lower the vapour isotope content from its initial (land) value at our site. The second estimate may explain why in the tropics δ_v of the sea breeze phase was higher than that of the land breeze phase (Lawrence et al., 2004).

3.4.3. The role of entrainment. Entrainment at the top of the boundary layer plays an important part in the vapour budget of the atmospheric boundary layer. The process can be viewed as a continuous exchange, through turbulent diffusion, of vapour between the drier free atmosphere above the boundary layer and the more moist boundary layer. In continental climate at mid-latitudes, the entrainment process can remove water vapour from the boundary layer at a rate comparable to the surface ET rate (Barr and Betts, 1997). Because vapour in the free atmosphere is much lighter, the process will cause the boundary layer vapour to become progressively lighter with time in daylight hours, as shown schematically in Fig. 1. At night, stable thermal stratification develops near the ground due to raidative cooling, effectively cutting off the surface air from the influence aloft.

The entrainment flux ^{18}O:^{16}O isotope ratio can be understood in terms of gradient diffusion. Assuming that ^{18}O and ^{16}O molecules diffuse with identical diffusivity across the capping inversion, the ^{18}O:^{16}O molar ratio, $R_{b,e}$, of the entrainment water vapour flux can be written as

$$R_{b,e} = \frac{w_m^{18} - w_f^{18}}{w_m^{16} - w_f^{16}} \tag{6}$$

where w_m^{16} and w_m^{18} are H_2 ^{16}O and H_2 ^{18}O mixing ratios in the mixed layer, and w_f^{16} and w_f^{18} are the mixing ratios in the free atmosphere. Equation (6) is rearranged to give the flux isotope ratio in δ notation

$$\delta_{b,e} = \delta_{v,m} + (\delta_{v,m} - \delta_{v,f})\frac{w_f^{16}}{w^{16} - w_f^{16}}, \tag{7}$$

where $\delta_{v,m}$ and $\delta_{v,m}$ are the vapour isotope ratios in the mixed layer and the free atmosphere, respectively.

So far very little information is available on the isotopic exchange at the boundary layer top. The study of He and Smith (1999) appears to be the only one that provides the complete data needed to evaluate eq. (7). According to their aircraft profiling in New England (their BLIP-04 experiment), the vapour mixing ratios were 3.2 and 0.14 g g^{-1} in the mixed layer and in the air layer above the inversion, respectively, and the vapour isotope ratios were -22 and -50 per mil in these two layers, respectively. This gives an entrainment flux isotope ratio of -20.7 per mil, or a discrimination factor

$$\Delta = \delta_{v,m} - \delta_{b,e} = -1.3 \text{ per mil}. \tag{8}$$

The change in the isotope ratio of the boundary layer vapour over time-step, Dt, is given by

$$\mathrm{D}(\delta_{v,m}) = \frac{F_{b,e}}{m}\,\Delta\,(\mathrm{D}t), \tag{9}$$

where $F_{b,e}$ is the $H_2{}^{16}O$ flux at the top of the boundary layer and m is total $H_2{}^{16}O$ mass per unit ground area in the boundary layer. Using the data reported by He and Smith (2001), and a typical value of 0.1 g m^{-2} s^{-1} for $F_{b,e}$, eq. (9) predicts a change of -0.8 per mil over 5 h, or about half of the peak-to-peak diurnal variation in the warm season. This supports the postulate that entrainment can change the vapour isotope ratio on a diurnal time scale. Additionally, according to eq. (9), the entrainment effect is more pronounced when the boundary layer is drier (lower m). This may be the reason why the diurnal pattern in δ_v was present at Great Mountain only on days of low humidity (Fig. 9b).

3.4.4. The role of evapotranspiration. In a model simulation of the exchange of ^{18}O in H_2O and CO_2 in a grassland, Riley et al. (2002) showed that the isotopic composition of soil evaporation could vary diurnally, with the lowest value of -17 per mil occurring at noon and the highest value of 10 per mil at night. In the simulation, δ_v was held at a constant value of -18 per mil. Thus the discrimination factor, Δ, was 1 and 28 per mil at noon and night, respectively. The diurnal variation was driven primarily by the change of relative humidity (W. J. Riley, 2005, personal communication). The overall effect on the vapour ^{18}O content in surface air in New England was probably very limited, for two reasons. First, in New England where much of the landscape is forested, the fraction of evaporation in ET is small, usually less than 5% (Black et al., 1996; Wilson et al., 2001). Secondly, the diurnal variation in the discrimination factor was out of phase with that of soil evaporation rate, that is, a relatively large daytime evaporation rate was associated with a Δ of small magnitude, and vice versa. As an order of magnitude estimate, using a rate equation similar to eq. (9), we estimate that the change in δ_v due to soil evaporation is less than 0.1 per mil over 5 h.

The isotopic content of transpiration is a subject of debate, with indirect evidence either supporting (Flanagan et al., 1991; Roden and Ehleringer, 1999) or challenging (Harwood et al., 1998; Cernusak et al., 2005) the assumption that, for time-scales of several hours or shorter, isotopic composition of transpiration is in a steady state and hence should be identical to that of soil water. Regardless of the validity of the steady-state assumption, transpiration should enrich the vapour in the surface layer with ^{18}O because the isotope ratio of the transpired water, which can be approximated by that of summer precipitation, was 10 per mil higher than the observed δ_v value (Table 1). The enrichment should increase δ_v continuously with time. Thus, transpiration will not cause a periodic pattern in δ_v.

3.5. Implication for the Keeling plot application

One potential application of the δ_v measurement is to infer the isotopic signal of the ET vapour flux using the Keeling plot approach. The Keeling plot takes the form

$$\delta_v = a + b/w, \tag{10}$$

where a and b are two regression constants. On the assumptions that temporal variations in δ_v and w are caused by ET only and that the isotopic signal of ET is constant over the observational period, the intercept parameter a is identical to the ET $^{18}O/^{16}O$ flux isotope ratio. According to the analysis presented here, this approach will encounter severe difficulty.

On time-scales of hours to days, much of the variation in δ_v is caused by the advection of airmass in varying stages of rainout history and has little to do with ET. The intercept parameter will depend on which part of the weather cycle is measured. Even in an idealized situation where the variation can be attributed to ET, there is reason to believe that the ET flux isotope ratio is not a constant. Further confounding the Keeling plot interpretation is the fact that the log-linear relationship predicted by the Rayleigh distillation theory (eq. 2), when plotted in the form of δ_v versus $1/w$, appears sufficiently linear if the change in w is less than two-fold. A linear fit to the Rayleigh curve will give an a value close to the typical precipitation isotope ratio found in the summer in mid-latitudes, which can be easily mistaken as the isotopic signature of ET. For these reasons, the intercept parameter of eq. (10) is generally an ambiguous quantity.

4. Conclusions

In this paper, the temporal variation in the vapour isotope ratio observed near the ground was examined in relation to various processes that operate on seasonal, weather cycle, rain shower and diurnal time-scales. Major conclusions are as follows.

(1) It is shown that on an annual time-scale, the vapour isotope ratio, δ_v, was a linear function of ln (w) and was approximated by a Rayleigh distillation model with partial (80%) rainout. The maximum and minimum observed hourly δ_v values were -10 and -38 per mil. On a monthly basis, the linear correlation coefficient with w was in the range 0.68–0.91. Temperature was not a good predictor for δ_v on temporal scales from days to weeks.

(2) On time-scales of a few days, considerable variation in δ_v was observed, often exceeding 20 per mil. Much of the variation was caused by advection of air mass in varying stages of rainout history through a weather cycle. When presented in a scatter plot of δ_v versus w, the data revealed a looping or hysteresis pattern: at a given moisture level, δ_v was higher in the wetting phase than in the drying phase of a weather cycle. The pattern was a common occurrence throughout the year.

(3) During rain events, vapour in the surface layer was in general brought to the state of equilibrium with the falling raindrops. In contrast, water vapour during snow storms was always heavier than the prediction of equilibrium, sometimes by as much as 15 per mil. The data indicate that the exchange of vapour with the falling snowflakes is too slow to bring the surface air to the equilibrium state.

(4) On a diurnal time-scale, a peak-to-peak variation of 2 and 1 per mil were observed at the coastal site (New Haven) in the warm and cold season, respectively, with lower value found in early afternoon hours, mostly due to land–sea breeze circulations. At the interior site (Great Mountain), evidence of a diurnal pattern was present only on days of low humidity, suggesting some role of boundary layer entrainment. According to mass balance consideration, evapotranspiration played a minor if not negligible role in the diurnal variations. The diurnal signal was an order of magnitude smaller than the variation associated with weather cycles.

(5) Given that much of the temporal variation in δ_v is caused by mechanisms that have little to do with ET, the intercept parameter of the Keeling plot is an ambiguous quantity and should not be interpreted as being equivalent to the isotopic signature of ET.

5. Acknowledgments

This work was supported by the US National Science Foundation through grants EAR-0229343 and DEB-0514904. We thank Kyounghee Kim for her assistance with the experiment and the Great Mountain Forest Corporation, Connecticut for its in-kind contribution that supports the field facility at the Great Mountain site.

6. Appendix A: Mathematical model for a two-phase system with partial rainout

Assuming that there is no mixing between the air within and outside the system, the liquid and vapour are in equilibrium and the precipitation leaving the system has the same isotopic composition as the liquid remaining in the system, Merlivat and Jouzel (1979) derived the following analytical model for the vapour $^{18}O/^{16}O$ molar ratio R_v

$$\frac{dR_v}{R_v} = \frac{(\alpha - 1)\, dn_v - n_l d\alpha}{n_v + \alpha n_l} \tag{A1}$$

where n_v and n_l are the number of moles of vapour and liquid water in the system, respectively. The amount of liquid water in the system is related to the rainout fraction, f, and the initial amount of water (all existing in the vapour form), n_o, as

$$n_l = (1 - f)(n_o - n_v) \tag{A2}$$

If α is assumed to remain constant, the integration eq. (A1) with respect to n_v, making use of eq. (A2), yields

$$\frac{R_v}{R_{v,o}} = \left\{ [1 - \alpha(1 - f)] \frac{n_v}{n_o} + \alpha(1 - f) \right\}^{(\alpha-1)/[1-\alpha(1-f)]}. \tag{A3}$$

where $R_{v,o}$ is the initial vapour $^{18}O/^{16}O$ molar ratio. Substituting n_v/n_o with w/w_o in eq. (A3) and converting to the δ notation, we obtain eq. (4).

References

Barr, A. B. and Betts, A. K. 1997. Radiosonde boundary layer budgets above a boreal forest. *J. Geophys. Res.* **102**, 29 205–29 212.

Black, T. A., den Hartog, G., Neumann, H. H., Blankan, P. D., Yang, P. C. co-authors. 1996. Annual cycles of water vapor and carbon dioxide fluxes in and above a boreal aspen forest. *Global Change Biol.* **2**, 219–229.

Cernusak, L. A., Farquhar, G. D. and Pate, J. S. 2005. Environmental and physiological controls over oxygen and carbon isotope composition of Tasmanian blue gum. *Eucalyptus globulus*. *Tree Physiol.* **25**, 129–146.

Cuntz, M., Ciais, P., Hoffmann, G. and Knorr, W. 2003. A comprehensive global three-dimensional model of δO^{18} in atmospheric CO_2: 1. Validation of surface processes. *J. Geophys. Res.* **108**, Art No 4527.

Craig, H. and Gordon, L. I. 1965. Deuterium and oxygen-18 variations in the ocean and the marine atmosphere. In: *Stable Isotopes in Oceanographic Studies and Paleotemperatures* (ed. E. Tongiorgi), Lab. di Geol. Necl., Pisa, Italy, 9–130.

Dongmann, G., Neurnberg, H. W., Forstel, H. and Wagener, K. 1974. On the enrichment of H_2 ^{18}O in leaves of transpiring plants. *Radiation and Environmental Biophysics* **11**, 41–52.

Ehhalt, D. H. and Östlund, H. G. 1970. Deuterium in Hurricane Faith 1966: preliminary results. *J. Geophys. Res.* **75**, 2323–2327.

Farquhar, G. D., Lloyd, J., Taylor, J. A., Flanagan, L. B., Syvertsen, J. P. co-authors. 1993. Vegetation effects on the isotope composition of oxygen in atmospheric CO_2. *Nature* **363**, 439–443.

Flanagan, L. B., Comstock, J. P. and Ehleringer, J. R. 1991. Comparison of modeled and observed environmental-influences on the stable oxygen and hydrogen isotope composition of leaf water in *Phaseolus-Vulgaris* L. *Plant Physiol.* **96**, 588–596.

Francey, R. J. and Tans, P. P. 1987. Latitudinal variation in oxygen-18 of atmospheric CO_2. *Nature* **327**, 495–497.

Gat, J. R., Klein, B., Kushnir, Y., Roether, W., Wernli, H. co-authors. 2003. Isotope composition of air moisture over the Mediterranean Sea: an index of the air-sea interaction pattern. *Tellus* **55B**, 953–965.

Gat, J. R. 1996. Oxygen and hydrogen isotopes in the hydrologic cycle. *Annu. Rev. Earth Planet. Sci.* **24**, 225–262.

Harwood, K. G., Gillon, J. S., Griffiths, H. and Broadmeadow, M. S. J. 1998. Diurnal variation of $\Delta^{13}CO_2$, $\Delta C^{18}O^{16}O$ and evaporative site enrichment of $\delta H_2{}^{18}O$ in *Piper aduncum* under field conditions in Trinidad. *Plant Cell and Environ.* **21**, 269–283.

He, H. 1998. *Stable Isotopes in the Evaporating Atmospheric Water Vapour*. PhD Dissertation, Yale University, New Haven, Connecticut, 234 p.

He, H. and Smith, R. B. 1999. Stable isotope composition of water vapour in the atmospheric boundary layer above the forests of New England. *J. Geophys. Res.* **104D**, 11657–11673.

He, H., Lee, X. and Smith, R. B. 2001. Deuterium in water vapour evaporated from a coastal salt marsh. *J. Geophys. Res.* **106**, 12 183–12 191.

Helliker, B. R., Roden, J. S., Cook, C. and Ehleringer, J. R. 2002. A rapid and precise method for sampling and determining the oxygen isotope ratio of atmospheric water vapor. *Rapid Commun. Mass Spectrom.* **16**, 9292–932.

Hoffmann, G., Werner, M. and Heimann, M. 1998. Water isotope module of the ECHAM atmospheric general circulation model: a study on timescales from days to several years. *J. Geophys. Res.* **103D**, 16 871–16 896.

Hu, X., Lee, X., Stevens, D. E. and Smith, R. B. 2002. A numerical study of nocturnal wavelike motion in forests. *Bound.-Layer Meteorol.* **102**, 199–223.

Jacob, H. and Sonntag, C. 1991. An 8-year record of the seasonal variation of ^2H and ^{18}O in atmospheric water vapor and precipitation at Heidelberg, Germany. *Tellus* **43B**, 291–300.

Jouzel, J., 1986. Isotopes in cloud physics: multiphase and multistage condensation processes. In: *Handbook of Environmental Isotope Geochemistry* Vol 2, (eds. B. P. Fritz, and J. C. Foutes), Elsevier Sci., New York, 61–112,

Keeling, C. D. 1958. The concentration and isotopic abundances of atmospheric carbon dioxide in rural and marine air. *Geochim. Cosmochim. Acta* **13**, 322–334.

Lai, C. T., Ehleringer, J. R., Bond, B. J. and Paw, U. K. T. 2005. Contributions of evaporation, isotopic non-steady state transpiration, and atmospheric mixing on the $\delta^{18}O$ of water vapor in Pacific Northwest coniferous forests. *Plant Cell and Environment* **29**, 77–94.

Lawrence, J. R., Gedzelman, S. D., Dexheimer, D., Cho, H. K., Carrie, G. D. co-authors. 2004. Stable isotopic composition of water vapour in the tropics. *J. Geophys. Res.* **109**, Art No D06115, doi10.1029/2003JD004046.

Lee, X. and Hu, X. 2002. Forest-air fluxes of carbon and energy over non-flat terrain. *Bound.- Layer. Meteorol.* **103**, 277–301.

Lee, X., Sargent, S., Smith, R. and Tanner, B. 2005. In-situ measurement of water vapour $^{18}O/^{16}O$ isotope ratio for atmospheric and ecological applications. *J. Atmos. Oceanic Tech.* **22**, 555–565.

Merlivat, L. and Jouzel, J. 1979. Global climatic interpretation of the deuterium-oxygen-18 relationship for precipitation. *J. Geophys. Res.* **84**, 5029–5033.

Pierrehumbert, R. T. 1999. Huascaran $\delta^{18}O$ as indicator of tropical climate during the last glacial maximum. *Geophys. Res. Letters* **26**, 1345–1348.

Riley, W. J. 2005. A modeling study of the impact of the delta O-18 value of near-surface soil water on the δO^{18} value of the soil-surface CO_2 flux. *Geochimica Et. Cosmochimica Acta* **69**, 1939–1946.

Riley, W. J., Still, C. J., Torn, M. S. and Berry, J. A. 2002. A mechanistic model of (H_2O)-O-18 and (CO_2)-O-18 fluxes between ecosystems and the atmosphere: Model description and sensitivity analyses. *Global Biogeochem. Cycles* **16**, Art No 1095.

Roden, J. S. and Ehleringer, J. R. 1999. Observations of hydrogen and oxygen isotopes in leaf water confirm the Craig-Gordon model under wide-ranging environmental conditions. *Plant Physiol.* **120**, 1165–1173.

Steward, M. K. 1975. Stable isotope fractionation due to evaporation and isotopic exchange of falling water drops: applications to atmospheric processes and evaporation of lakes. *J. Geophys. Res.* **80**, 1133–1146.

Sturm, K., Hoffmann, G., Langmann, B. and Stichler, W. 2005. Simulation of delta O-18 in precipitation by regional circulation model REMOiso. *Hydrol. Process.* **19**, 3425–3444.

White, J. W. C. and Gedzelman, S. D. 1984. The isotope composition of atmospheric water vapor and the concurrent meteorological conditions. *J. Geophys. Res.* **89**, 4937–4939.

Williams, D. G., Cable, W., Hultine, K., Hoedjes, J. C. B., Yepez, E. A. co-authors. 2004. Evapotranspiration components determined by stable isotope, sap flow and eddy covariance techniques. *Agric. For. Meteorol.* **125**, 241–258.

Wilson, K. B., Hanson, P. J., Mulholland, P. J., Baldocchi, D. D. and Wullschleger, S. D. 2001. A comparison of methods for determining forest evapotranspiration and its components: sap-flow, soil water budget, eddy covariance and catchment water balance. *Agric. For. Meteorol.* **106**, 153–168.

Zielinski, G. A. and Keim, B. D. 2003. *New England Weather, New England Climate*. University Press of New England, Lebanon, New Hampshire, 276 p.